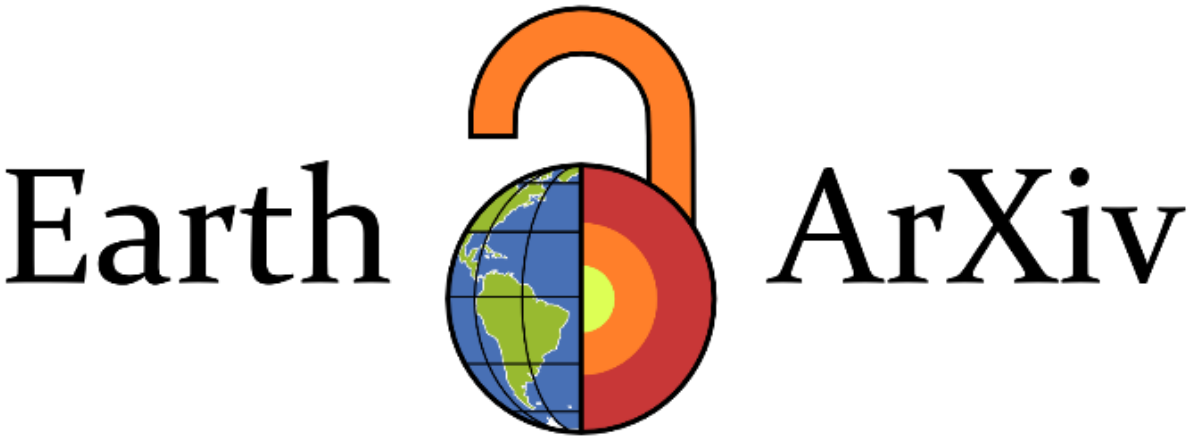

Improving sub seasonal streamflow prediction for hydrological drought forecasting using machine learning in the Rhine River basin in the Netherlands

Tefera Brhanu Shibeshi [1,3,4], **Shankar karuppannan** [2,5]

[1]School of Civil Engineering and Architecture, Adama Science and Technology University, Adama, Ethiopia
[2] Department of Applied Geology, College of Applied Natural Sciences, Adama Science and Technology University, Adama, Ethiopia
[3]Hydro Informatics Department, IHE Delft Institute for Water Education, Westvest 7, 2611 AX Delft, Netherlands
[4]Civil and Environmental Engineering Department, College of Engineering, Villanova University, PA, USA
[5]Department of Research Analytics, Saveetha University, Chennai-600077, Tamil Nadu,India.
*Corresponding author: E-mail: tefixbrhan@gmail.com

Abstract

Accurate sub-seasonal streamflow forecasts are essential for hydrological drought preparedness in large river basins with competing water demands. Traditional process-based hydrological models often struggle to represent non-linear, non-stationary catchment behavior under changing climate and land-use conditions. In this study, we develop Long Short-Term Memory (LSTM) networks to improve sub-seasonal streamflow forecasting in the Rhine River Basin, focusing on low-flow conditions at the Lobith outlet in the Netherlands. We evaluate several univariate and multivariate LSTM configurations that ingest combinations of streamflow from multiple upstream gauges and basin-average precipitation and temperature derived from GRDC and ERA5 data. Models are trained to predict daily discharge, weekly averages, and weekly minimum flows for lead times of 1–20 days and 1–4 weeks, and forecast skill is assessed using the Nash–Sutcliffe efficiency (NSE) and mean absolute percentage error (MAPE) relative to climatological benchmarks. The best multivariate LSTM model achieves NSE values up to 0.99 at short lead times and substantially reduces MAPE compared with climatology, particularly for drought-relevant low-flow metrics, while predictive skill gradually declines as the forecast horizon increases. These results highlight the potential of deep learning to enhance sub-seasonal low-flow forecasting and support early-warning systems for hydrological drought risk management in large European river basins.

Keywords: Deep learning, sub-seasonal forecasting, streamflow prediction, low-flow conditions, hydrological drought, Rhine River Basin, ERA5 reanalysis.

Introduction

Drought is a prolonged period of below-average precipitation or water availability in a particular region, leading to water scarcity and adverse impacts on ecosystems, agriculture, water supplies, and other components of human and natural systems [1]. Among the various types of droughts,

hydrological droughts are characterized by sustained reductions in streamflow and groundwater levels resulting from persistent precipitation deficits [2]. Consequently, streamflow serves as a vital indicator of hydrological drought and is integral to maintaining ecosystem health and supporting human livelihoods. Accurate prediction of streamflow is crucial for effective water resources management, the development of early-warning systems, and the mitigation of drought-related risks, particularly in the context of increasing climate variability.

Historically, streamflow forecasting has predominantly relied on process-based hydrological models that simulate watershed dynamics through physical equations and conceptual parameters. Despite substantial advances, such models frequently encounter challenges in accurately representing the non-linear and non-stationary behavior of hydrological systems under evolving climatic and land-use conditions [7]. Issues such as parameter uncertainty, structural limitations, and the complexity of representing heterogeneous catchment processes can reduce predictive accuracy, especially during extremes. Ensemble forecasting methodologies have been introduced to address predictive uncertainty, but they often require substantial computational resources and involve intricate probabilistic evaluations, which may constrain their operational applicability [8-9].

In recent years, machine-learning (ML) techniques have emerged as powerful alternatives for hydrological forecasting. These data-driven approaches can capture hidden patterns and non-linear relationships between meteorological variables and streamflow without requiring explicit knowledge of the underlying physical processes [12;11;10;14]. Among them, Long Short-Term Memory (LSTM) networks, a variant of recurrent neural networks introduced to overcome vanishing and exploding gradient problems [15], have demonstrated particular proficiency in modelling long-term temporal dependencies in hydrological time series. Numerous studies [12,16–18] have shown that LSTM models can outperform traditional hydrological and statistical models in simulating complex rainfall–runoff dynamics across diverse catchments and temporal scales.

However, several important gaps remain. First, many existing LSTM applications in hydrology have focused on daily or event-based flows, with limited emphasis on sub-seasonal lead times that are particularly relevant for hydrological drought preparedness. Second, low-flow and minimum-flow conditions, which directly affect navigation, water supply, and ecological integrity, have received less attention than peak flows in the deep-learning literature. Third, the integration of multi-gauge discharge records with basin-scale meteorological forcings from modern reanalysis products, such as ERA5, for sub-seasonal low-flow prediction in large European river basins has not yet been comprehensively explored.

The Rhine River is one of Europe's most important rivers, supporting navigation, industry, agriculture, and ecosystems across several countries [3]. Its lower reach at Lobith, on the Dutch German border, is a key control point for water allocation and drought management in the downstream delta. Recent low-flow events have highlighted the vulnerability of navigation and water-supply sectors to prolonged reductions in discharge, underscoring the need for more skillful sub-seasonal forecasts of low-flow conditions [3-4]. Developing robust data-driven forecasting tools for the Rhine therefore has both scientific and practical relevance.

Building upon this background, the present study aims to enhance medium-range, sub-seasonal streamflow prediction for the Rhine River, with lead times extending up to one month, with a particular focus on hydrological drought conditions at the Lobith outlet. Specifically, we examine both univariate (streamflow-only) and multivariate (streamflow combined with meteorological predictors such as precipitation and temperature) LSTM input configurations to evaluate how varying temporal resolutions (daily and weekly) impact model performance. By employing stacked LSTM architectures with optimized hyperparameters, we seek to improve low-flow forecasting accuracy and to assess the operational applicability of data-driven models for hydrological drought monitoring in a large European river basin.

This study extends previous work on low-flow prediction in the Rhine and on LSTM-based hydrological forecasting in three ways. First, it targets sub-seasonal lead times up to one month, explicitly focusing on both daily and weekly minimum flows that are directly relevant for hydrological drought management. Second, it evaluates multivariate LSTM configurations that integrate multiple upstream gauge records with basin-average meteorological predictors from ERA5, thereby exploiting both hydrological routing and meteorological memory. Third, it systematically compares model performance against climatological benchmarks across multiple years and lead times, with emphasis on low-flow conditions, to identify practically useful forecast horizons and remaining limitations.

Materials and methods

Study area and data

The Rhine River is a major European waterway that connects industrial regions to global markets via the Port of Rotterdam. The river extends from alpine headwaters at elevations of up to 4000 m to approximately 6 m below sea level in the Netherlands, with a total length of about 1233 km and a drainage area of roughly 185,000 km² supporting nearly 60 million inhabitants [2]. In its main course, the Rhine flows from Switzerland through Germany, enters the Netherlands at Lobith, and ultimately discharges into the North Sea.

The hydrological regime of the Rhine Basin is shaped by a temperate climate with strong intra- and interannual variability, making the basin susceptible to both floods and prolonged low-flow conditions [4]. In the Rhine Delta, monthly mean discharges below approximately 1100 $m^3 s^{-1}$ are considered hydrological droughts and can lead to substantial economic impacts on navigation and water supply [5].

To capture the hydroclimatic controls on streamflow, this study primarily used streamflow observations from major Rhine main-stem gauges. Long historical records are available at Basel and Maxau in the Upper Rhine, Kaub and Worms in the Middle Rhine, and Lobith and Kolen in the Lower Rhine (Figure 1). Streamflow data were obtained from the Global Runoff Data Centre (GRDC), with daily records covering 1980–2021 for Lobith and 1980–2018 for Basel and the other upstream gauges (Table 1).

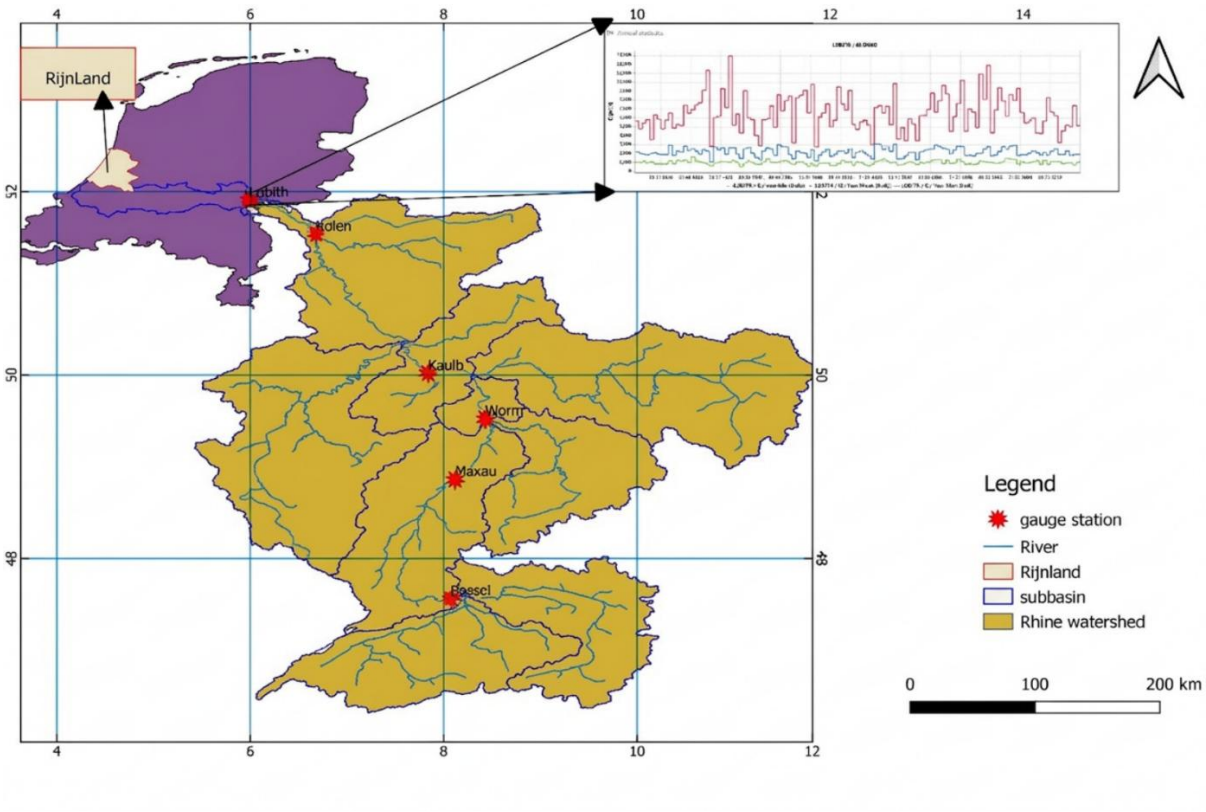

Figure 1 Map of the Rhine River catchment and the Netherlands

Research framework

We designed a four-step workflow to develop and evaluate LSTM-based sub-seasonal streamflow forecasts at the Lobith outlet:

Data selection and preprocessing: - compilation and quality control of streamflow and meteorological datasets, feature selection, and temporal standardization.

Model development and training: - design of LSTM architecture, hyperparameter tuning, and training with early stopping.

Model testing: - out-of-sample performance assessment for different lead times and temporal resolutions.

Performance evaluation and analysis: - comparison with climatological benchmarks and detailed analysis of low-flow conditions.

The following subsections describe each step in detail.

Data selection and preprocessing

2.3.1. Streamflow data

Daily discharge time series from the main Rhine gauges (Basel, Maxau, Kaub, Worms, Kolen, and Lobith) were obtained from the GRDC [24]. For each gauge, we selected the longest continuous period with minimal missing data between 1980 and 2018 (1980–2021 for Lobith). Minor gaps were infilled using simple linear interpolation, while periods with extensive missing values were excluded from modelling.

Table 1 Gauge stations for streamflow observations used as inputs for the LSTM model

Gauge station	Period	Temporal resolution
Lobith	1980-2021	daily
Worm	1980-2019	daily
Maxau	1980-2019	daily
Kolen	1980-2019	daily
Kaulb	1980-2019	daily
Basel	1980-2018	daily

2.3.2. Meteorological data

Meteorological predictors were derived from the ERA5 reanalysis produced by the European Centre for Medium-Range Weather Forecasts (ECMWF). We used 6-hourly total precipitation and 2 m air temperature fields at 0.25° × 0.25° spatial resolution for 1980–2018 [20]. For each time step, grid cells intersecting the Rhine Basin were identified and used to compute basin-average precipitation and temperature time series. This spatial averaging reduces grid-scale noise and ensures consistency between meteorological forcings, and streamflow observed at the basin outlet, as recommended by previous studies on ERA5-driven hydrological modelling [21-22]. Daily basin-average series were obtained by summing precipitation and averaging temperature over the 6-hourly records.

2.3.3. Quality control, alignment, and splitting

All-time series were checked for duplicates, formatting errors, and outliers. After quality control, streamflow and meteorological datasets were temporally aligned to a common daily time axis. To facilitate sub-seasonal forecasting, daily series were aggregated to weekly averages and weekly minima, providing predictors and targets at multiple hydrologically meaningful

timescales. The aligned dataset was then split into training (60%), validation (30%), and test (10%) sets, using contiguous time blocks to preserve temporal dependence.

Normalization

To stabilize training and improve convergence, all input variables were scaled to the [0,1] range using min–max normalization applied to the training period. For a given variable, the normalized value Q_i was computed from the raw value $Q_{i,\text{actual}}$ as

$$\mathrm{Q_i} = \frac{(\mathrm{Q_{i,actual}} - \mathrm{Q_{i,min}})}{(\mathrm{Q_{f,max}} - \mathrm{Q_{f,min}})} \qquad (1)$$

where $Q_{i,\text{min}}$ and $Q_{i,\text{max}}$ denote the minimum and maximum of that variable in the training set. After prediction, normalized outputs were transformed back to physical units using

$$\mathrm{Q_{i,actual}} = \mathrm{Q_{i(n)}}\big(\mathrm{Q_{i,max}} - \mathrm{Q_{i,min}}\big) + \mathrm{Q_{i,min}} \qquad (2)$$

ensuring consistency between model outputs and observed streamflow.

LSTM network formulation

Long Short-Term Memory (LSTM) networks are a class of recurrent neural networks specifically designed to model long-range temporal dependencies while mitigating vanishing and exploding gradient problems [15]. An LSTM cell maintains an internal memory state c_t and a hidden state h_t, which are updated at each time step (t) using a set of gating mechanisms [19]. Given an input vector x_t and previous hidden and cell states (h_{t-1}, c_{t-1}), the gates are defined as

$$f_t = \sigma\big(W_{fx}x_t + W_{fh}h_{t-1} + b_f\big) \qquad (4)$$

$$o_t = \sigma(W_{ox}x_t + W_{oh}h_{t-1} + b_o) \qquad (5)$$

where i_t, f_t, and o_t are the input, forget, and output gates, respectively; (W) and (b) denote trainable weight matrices and bias vectors; and $\sigma(\cdot)$ is the logistic sigmoid activation. The candidate cell update $\tilde{c}_t$ and the new cell and hidden states are computed as

$$c_t = f_t \odot c_{t-1} + i_t \odot \tilde{c}_t \qquad (7)$$

$$h_t = o_t \odot \tanh(c_t) \qquad (8)$$

where $\tanh(\cdot)$ is the hyperbolic tangent activation, and $\odot$ denotes element-wise multiplication. The network output y_t at time (t) is obtained from the hidden state via a dense (fully connected) layer.

where W_y and b_y are the output weights and bias. In this study, sequences of lagged inputs $X = \{x_{t-n+1}, \dots, x_t\}$ are used to predict streamflow at lead times of up to four weeks. The complete architecture is illustrated in Figure 1A.

LSTM implementation and hyperparameter tuning

To predict streamflow, we considered sequences of lagged inputs $X = (Q_{t-n+1}, \dots, Q_t)$ for univariate experiments and $X = (Q_{t-n+1}, \dots, Q_t, P_{t-n+1}, \dots, P_t, T_{t-n+1}, \dots, T_t)$ for multivariate experiments, where (Q) is streamflow, (P) precipitation, (T) temperature, and (n) is the window size.

We used stacked LSTM architectures with two hidden layers and a final dense output layer. Key hyperparameters included the number of units in each LSTM layer, batch size, learning rate, window size, and number of epochs. Initial ranges for these hyperparameters were selected based on preliminary experiments and previous hydrological deep-learning studies [12;19;7]. Hyperparameter tuning was performed using the Keras Tuner library with a grid search strategy, optimizing the mean squared error (MSE) on the validation dataset. The optimized configurations for univariate and multivariate models are summarized in Table 3. The overall experimental setup is illustrated in the graphical representation in Figure 2A in Appendix.

Software and computational environment

All models were implemented in Python (version 3.10) using TensorFlow (version 2.15) and Keras (version 2.15), with hyperparameter tuning performed via Keras Tuner (version 1.4.3). Training and evaluation were conducted in the Google Colab environment on an NVIDIA T4 GPU with 16 GB of RAM. Random seeds were fixed for NumPy and TensorFlow to enhance reproducibility and early stopped monitoring the validation loss to prevent overfitting.

2.10. Model training and validation

After standardization and splitting, models were trained on the training set and monitored on the validation set. Early stopping was configured to halt training when the validation loss (MSE) did

not improve for 20 consecutive epochs. The best model weights, corresponding to the minimum validation loss, were retained. The final model performance was evaluated on the independent test set, which was not used during training or hyperparameter tuning. For each configuration, we trained the model multiple times with different random seeds and selected the run with the best validation performance, while also inspecting consistency across runs.

2.11. Experimental configurations

We evaluated a set of single-input single-output (SISO) and multiple-input single-output (MISO) LSTM configurations at daily and weekly timescales (Table 2). SISO experiments used only Lobith streamflow as input, whereas MISO experiments combined Lobith with upstream gauges and/or basin-average precipitation and temperature. Daily models predicted daily discharge or daily minimum at lead times of 1, 3, 5, 10, 15, and 20 days. Weekly models predicted weekly averages or weekly minima at lead times of 1–4 weeks. Window sizes of 30 and 365 days (or 4 and 52 weeks) were selected based on autocorrelation and cross-correlation analyses to capture short-term memory and annual cycle effects.

Table 2 Configuration of the experiments

Input types	Configuration		Input variables	Temporal resolution	Output variables	Leadtime(t)	Window size	Data used	
Univariate	SISO	**Exp#1**	Q	daily	Qt+1	0,3,5,10,15,20	30,365	Q_Lobith	
	SISO	**Exp#2**	Q	Weekly average	Qt+1	0,1,2,3	4,52		
	SISO	**Exp#3**	Q	Weekly minimum	Qt+1	0,1,2,3	4,52		
Multivariate	MISO	**Exp#1**	Q	daily	Qt+1	0,3,5,10,15,20	30	Q_Lobith	Q_Maxau
	MISO	**Exp#2**	Q	daily	Qt+1	0,3,5,10,15,20	30	Q_Lobith	Q_Koln
	MISO	**Exp#3**	Q	daily	Qt+1	0,3,5,10,15,20	30	All Qi	
	MISO	**Exp#4**	Q, P, T	daily	Qt+1	0,3,5,10,15,20	30,365	All gauges Qi, Precipitation & Temp	
	MISO	**Exp#5**	Q, P, T	Weekly minimum	Qt+1	0,1,2,3	4	All gauges Qi, Precipitation & Temp	

***SISO** -single input single output ***SIMO** -single input multiple output

***MISO**-multiple input single output ***Exp**-Experiment

2.12. Performance metrics

Model performance was evaluated using the mean absolute percentage error (MAPE) and Nash–Sutcliffe efficiency (NSE), computed between predicted and observed streamflow on the test set. MAPE is defined as

$$MAPE = \frac{1}{N}\sum_{i=1}^{N} \left| \frac{Q_i - Q_p}{Q_i} \right| \times 100 \qquad (8)$$

where (N) is the number of test samples, Q_i is the observed streamflow at time (i), and Q_p is the corresponding model prediction. Lower MAPE values indicate more accurate predictions. NSE measures the proportion of the variance in the observations explained by the model and is defined as

$$NSE = 1 - \frac{\sum_{i=1}^{N}(Q_i - Q_p)^2}{\sum_{i=1}^{N}(Q_i - \bar{Q})^2} \qquad (9)$$

where $\bar{Q}$ is the mean observed streamflow over the test period. NSE ranges from $-\infty$ to 1, with values close to 1 indicating high predictive skill, values near 0 indicating performance similar to the mean of the observations, and negative values indicating performance worse than the mean [12].

Results and Discussion

Input variables and window sizes that lead to best model

Based on the correlation analysis with a threshold of 50%, basin-average precipitation and temperature from ERA5 emerged as the dominant meteorological predictors for streamflow at Lobith, alongside upstream discharge from Basel, Maxau, Kaub, Worms, and Kolen. When these variables were incorporated into the multivariate LSTM configurations, they consistently improved predictive performance relative to models driven by Lobith streamflow alone.

Autocorrelation analysis of the Lobith discharge series suggested an effective memory of approximately 30 days, which motivated the use of a 30-day window for daily models. Cross-correlation analyses between Lobith and upstream gauges, as well as between Lobith and basin-average precipitation and temperature, indicated that both a 30-day window and a 365-day window (to capture the annual hydrological cycle) were informative [21]. Consequently, we evaluated configurations with window sizes of 30 and 365 days (and 4 and 52 weeks for weekly models) to represent short-term and seasonal memory, respectively

Hyper parameter tuning

The Keras Tuner search identified stacked LSTM architectures with two hidden layers as a good compromise between flexibility and computational cost. For both univariate and multivariate models, an LSTM architecture with 64 units in the first layer and 50 units in the second layer, followed by a dense output node, yielded robust performance (Table 3). Rectified Linear Units (ReLU) were used as activation functions in the LSTM layers, while the Adam optimizer with a learning rate of 0.001 was adopted for training.

The optimal batch sizes differed between setups: a batch size of 32 provided stable training for univariate models, whereas a batch size of 64 improved efficiency and convergence for multivariate models without degrading accuracy. Early stopping prevented overfitting by halting training when the validation loss no longer improved, and the final models achieved low training and validation MSE, indicating that the architectures were well-matched to the complexity of the forecasting tasks.

Table 3. Final optimized hyperparameters for univariate and multivariate LSTM models.

Hyperparameter	Univariate Model	Multivariate Model	Description
Number of LSTM Layers	2	2	Two stacked LSTM layers selected after tuning
Hidden Units (Layer 1 / Layer 2)	64 / 50	64 / 50	Optimized configuration identified via Keras Tuner
Activation Function	ReLU	ReLU	Rectified Linear Units for nonlinear transformation
Optimizer	Adam	Adam	Adaptive moment estimation algorithm
Learning Rate	0.001	0.001	Default Adam learning rate used for stable convergence
Batch Size	32	64	Smaller batch favored univariate stability; larger for multivariate efficiency
Epochs	500	1000	Early stopping applied to prevent overfitting
Loss Function	Mean Squared Error (MSE)	Mean Squared Error (MSE)	Consistent metric for both experiments
Input Window Size	30 timesteps	365 timesteps	Optimal lag-window configuration for each setup
Output Layer	Dense (1)	Dense (1)	Single-node output for regression prediction

1.1. Comparison of model prediction performance with climatology prediction

The predictive performance of the best daily (Exp#4) and weekly minimum (Exp#5) models was benchmarked against climatological forecasts using the independent test sets. For the daily configuration, Exp#4 achieved NSE values decreasing from 0.99 at a lead time of 1 day to 0.47 at a lead time of 20 days, indicating that the model captured a substantial portion of the observed variance even at longer horizons. In contrast, the climatological baseline exhibited an NSE of only 0.15 over the same period, highlighting its limited skill. MAPE values for Exp#4 were as low as 4% at a 1-day lead time and increased gradually with lead time, whereas the climatological predictions had a MAPE of 51.1%, reflecting large systematic errors (Figures 2 and 3).

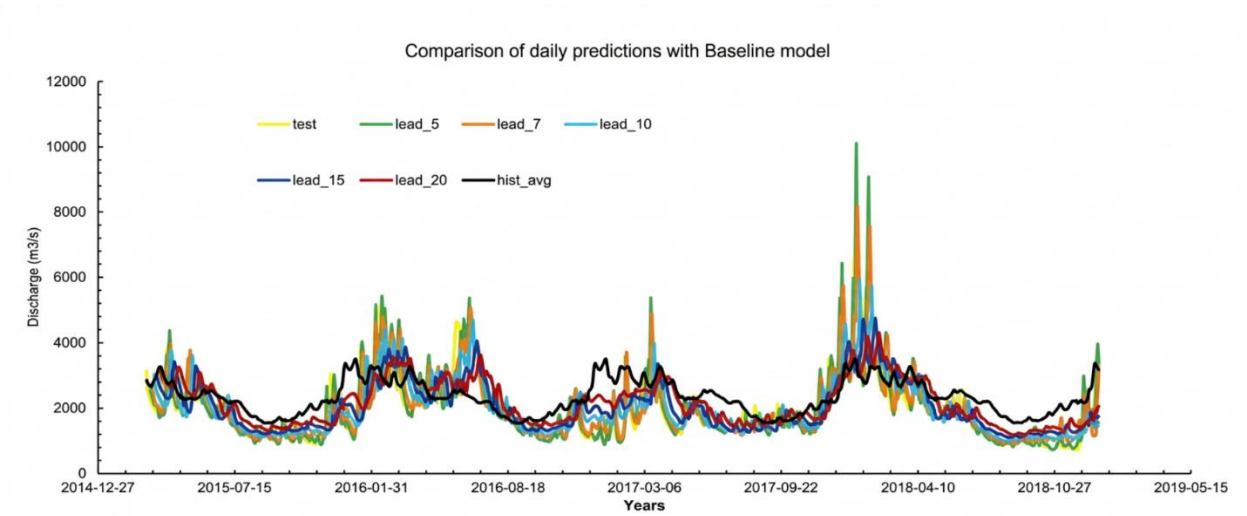

Figure 2. Comparison between observed daily discharge and predictions generated by the LSTM model at various forecast lead times (5, 7, 10, 15, and 20 days), alongside the climatological baseline. This figure demonstrates the model's proficiency in replicating daily flow variability, encompassing both high- and low-flow periods, across different prediction horizons.

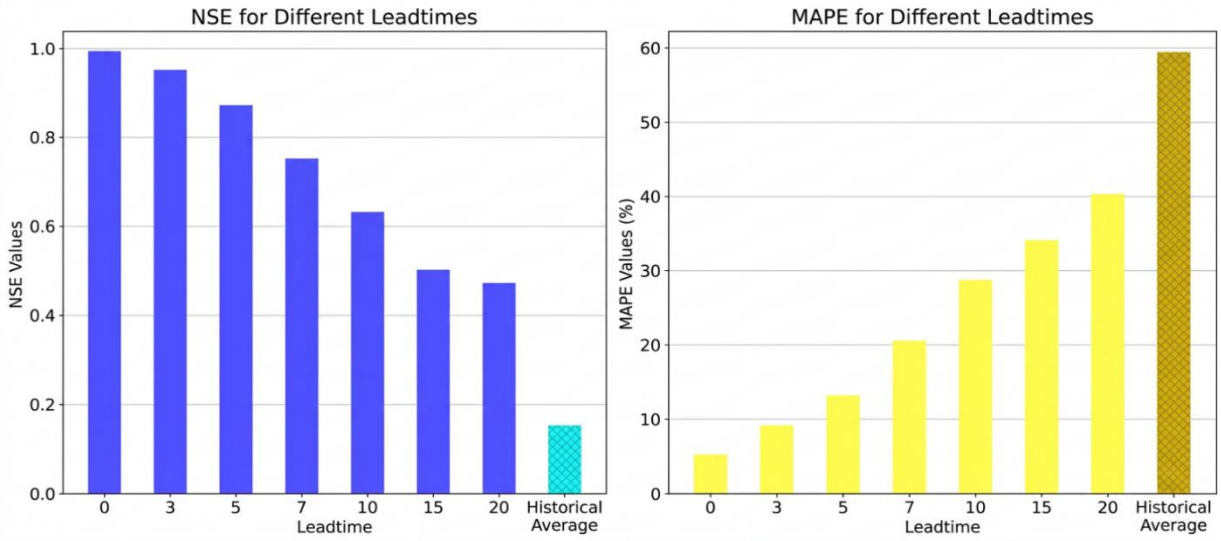

Figure 3. Comparison of model performance based on the Nash–Sutcliffe Efficiency (NSE) and Mean Absolute Percentage Error (MAPE) metrics for daily LSTM predictions at different lead times (0, 3, 5, 7, 10, 15, and 20 days) and the climatological baseline. The results show that the NSE values decrease and the MAPE values increase with longer forecast horizons, reflecting a gradual reduction in predictive accuracy over time.

For the weekly minimum forecasts (Exp#5), the LSTM models also outperformed climatology. At a 1-week lead time, NSE reached 0.88 with MAPE of 9.68%, while the climatological benchmark had an NSE of 0.15 and MAPE of 41.6%. At a 2-week lead time, the model retained reasonable skill, with NSE of 0.63 and MAPE of 17.91%, again substantially better than climatology. Beyond 2 weeks, NSE values declined and MAPE increased, indicating a progressive loss of skill with increasing forecast horizon (Figures 4 and 5).

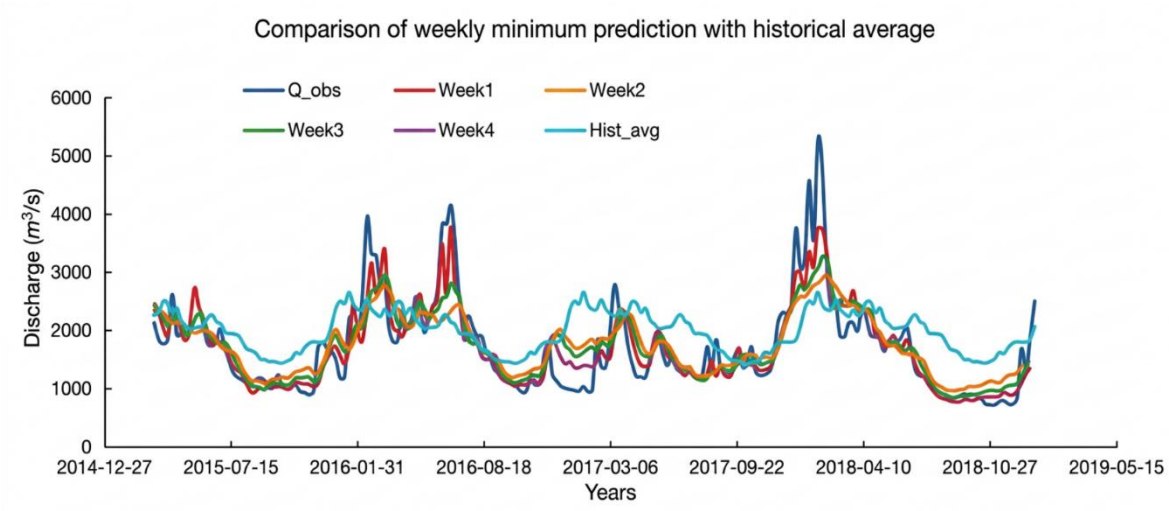

Figure 4. Comparison between observed discharge and LSTM model predictions of weekly minimum flows across different forecast lead times (1–4 weeks), together with the climatological baseline. The results show that the LSTM model successfully reproduced the timing and magnitude of low-flow conditions while maintaining coherence with the observed hydrograph patterns.

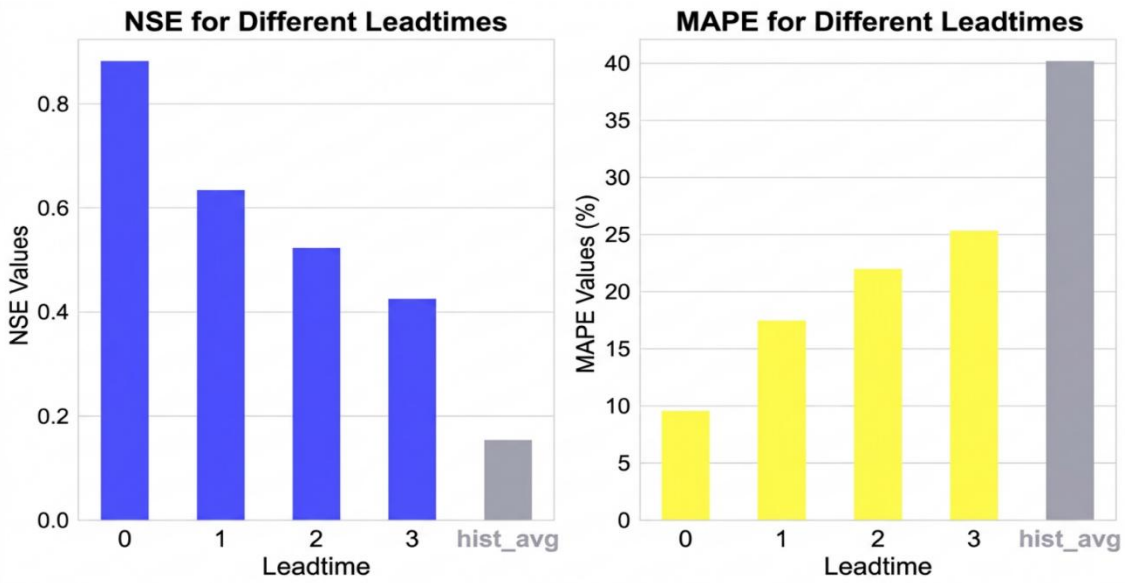

Figure 5. Comparison of model performance based on the Nash–Sutcliffe Efficiency (NSE) and Mean Absolute Percentage Error (MAPE) metrics for weekly LSTM predictions at different lead times (0–3 days) and the climatological baseline. The results indicate that the NSE decreases and the MAPE increases with increasing lead time, reflecting a gradual decline in predictive skill as the forecast horizons extend.

The Taylor diagrams (Figure 6) summarize these differences in terms of correlation coefficient, standard deviation, and root-mean-square difference relative to observations. In both daily and weekly minimum experiments, the LSTM predictions cluster closer to the observed reference point and the reference standard deviation line than the climatological forecasts, confirming their superior ability to reproduce the magnitude and variability of streamflow across a range of lead times.

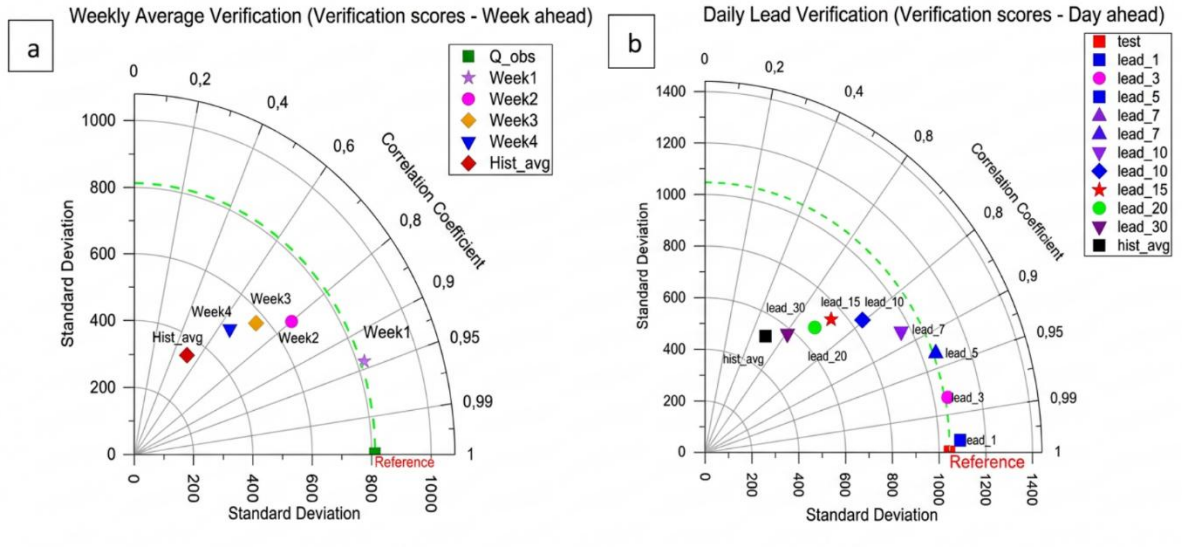

Figure 6. Taylor diagram illustrates the comparative performance of the best LSTM model predictions and the climatological baseline. Panel (a) presents the results for the weekly minimum discharge under Exp#5, and panel (b) shows the results for the daily discharge under Exp#4. The diagrams summarize the model performance in terms of the correlation coefficient, standard deviation, and root-mean-square difference relative to the observations. In both cases, the LSTM models exhibited higher correlation and lower error than the climatological reference, confirming their improved ability to reproduce observed flow variability across different temporal scales.

1.2.Low-flow prediction performance

To evaluate performance under hydrological drought conditions, we focused on the lowest 25% of observed streamflow values and compared the corresponding LSTM predictions and climatology. For daily minimum low flows aggregated by year, the model achieved positive NSE values and low MAPE (typically below 5%) at short lead times (0–3 days) across 2015–2018, indicating good correspondence with observed minima. However, as lead time increased to 5, 7, 15, and 20 days, NSE values decreased markedly and became strongly negative in some years, while MAPE increased, showing that the model could perform worse than the mean of the observations at extended horizons (Table 4a).

Table 4 summarizes the NSE and MAPE values for the weekly and daily minimum low flow predictions from 2015 to 2018.

(a). Daily minimum low-flow prediction metrics (2015–2018)

Lead-time (days)	**2015**		**2016**		**2017**		**2018**	
	(NSE)	(MAPE %)	(NSE)	(MAPE %)	(NSE)	(MAPE %)	(NSE)	(MAPE %)
0	0.82	2.3	0.90	3.1	0.86	2.8	0.91	3.2
3	0.74	4.6	0.70	5.4	0.72	4.3	0.88	6.0
5	0.68	7.8	−1.1	10.2	0.61	10.6	−5.8	11.5
7	−1.25	10.5	−800	25.7	−2100	22.8	−15	25.4
15	−920	58.4	−2600	56.3	−58000	71.9	−80	58.3
20	−3200	108.6	−3000	102.4	−110000	136.7	−120	105.9
Hist. avg	−3400	112.7	−3100	108.1	−135000	220.5	−190	109.8

*0 stands for lead time a day ahead

(b) weekly Minimum Flow Prediction (Aggregated 2015–2018)

Lead time (weekly)	**NSE**	**MAPE (%)**
Week 1	0.96	7.2
Week 2	0.82	9.5

Week 3	−0.5	24.1
Week 4	−43.8	38.7
Hist. avg	−220	92.4

Weekly minimum low-flow forecasts aggregated over 2015–2018 exhibited a similar pattern. The LSTM model attained high skill at short lead times (NSE = 0.96 and MAPE = 7.2% at week 1; NSE = 0.82 and MAPE = 9.5% at week 2), but NSE dropped to −0.5 and −43.8 for weeks 3 and 4, respectively, with corresponding MAPE values of 24.1% and 38.7% (Table 4b). These results indicate that LSTM forecasts add clear value over climatology for low-flows at lead times up to roughly 1–2 weeks, whereas their utility diminishes substantially at longer horizons.

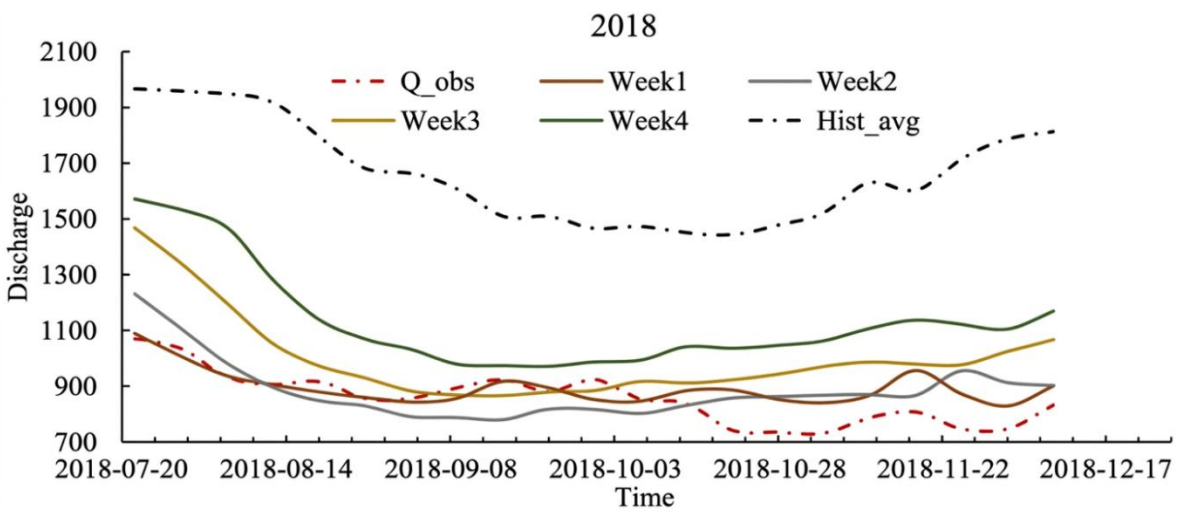

Figure 7. Comparison of observed and LSTM-predicted weekly minimum discharges during the 2018 low-flow period, together with the climatological baseline. The figure illustrates that the LSTM model accurately reproduces both the timing and magnitude of the observed low flows across different forecast lead times (1–4 weeks). Compared with the climatological prediction, the LSTM forecasts better captured the decline and recovery patterns of streamflow, highlighting the model's capacity to simulate hydrological persistence and improve low flow forecasting for drought monitoring and sustainable water resource management.

Time series comparisons for the 2018 low-flow period at Lobith further illustrate these findings. For weekly minima, the LSTM model reproduced both the timing and magnitude of low-flow events more accurately than the climatological baseline, capturing the onset, persistence, and partial recovery of drought conditions across successive weeks (Figure 7). For daily flows, the model likewise captured the timing and variability of low flows more effectively than climatology at short lead times, but differences grew as the forecast horizon extended (Figure 8). Overall, the analysis suggests that LSTM-based forecasts provide actionable low-flow

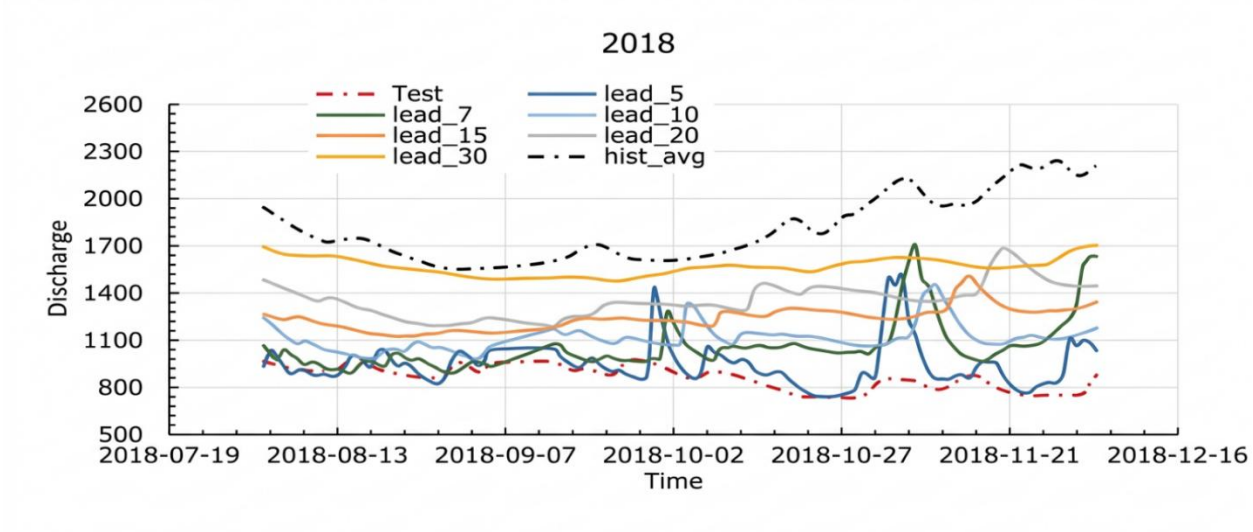

information at short sub-seasonal horizons, while caution is warranted for longer lead times.

Figure 8. Comparison of observed discharge and LSTM-predicted daily flows during the 2018 low-flow period across different forecast lead times (5, 7, 10, 15, 20, and 30 days), along with the climatological baseline. The figure shows that the LSTM model captures the timing and variability of the observed low flows more effectively than the climatological prediction, particularly for shorter lead times. The improved alignment of model predictions with observed discharge highlights the LSTM's ability to learn temporal dependencies and enhance short-term low flow forecasting accuracy, contributing to more reliable drought preparedness and sustainable water resource planning.

1.3.Limitations and implications for operational use

While the proposed LSTM configurations show promising performance, several limitations must be acknowledged. First, the reliability of ERA5 forcing data remains a significant source of uncertainty. Reanalysis products can smooth spatial and temporal variability and exhibit systematic biases in precipitation and temperature, particularly in complex orographic regions [21;22]. Such biases may propagate non-linearly into streamflow simulations, especially under low-flow conditions where errors in rainfall or evapotranspiration forcings can have amplified impacts [23].

Second, the transferability of data-driven models is inherently limited: relationships learned for the Rhine may not generalize directly to basins with different hydroclimatic or physiographic

characteristics without careful recalibration or domain adaptation [7]. Third, although the computational cost of individual LSTM forecasts is low once trained, the development of the long training runs, extensive hyperparameter tuning, and ensemble experimentation—requires substantial computational resources, which may constrain real-time operational deployment in some settings [25].

Despite these limitations, the results demonstrate that LSTM-based models can significantly improve sub-seasonal low-flow forecasts relative to simple climatological benchmarks, particularly at lead times of up to 1–2 weeks. In the context of the Rhine River, such forecasts could support more informed navigation management, water allocation, and drought contingency planning. Future work should explore bias-corrected or multi-model forcings, domain-adaptable architectures, and hybrid physics–data approaches to further enhance robustness and generalization of low-flow forecasting systems.

2. Conclusions and recommendations

This study evaluated stacked Long Short-Term Memory (LSTM) networks for sub-seasonal streamflow forecasting in the Rhine River Basin, with a focus on hydrological drought conditions at the Lobith outlet. Using daily discharge from multiple main-stem gauges and basin-average precipitation and temperature from ERA5, we developed and tested several univariate and multivariate LSTM configurations at daily and weekly timescales. Hyperparameter tuning showed that two-layer LSTM architectures with 64 and 50 units, respectively, provided a good balance between predictive skill and computational cost.

The multivariate configurations that integrated upstream discharge and basin-average meteorological forcings consistently outperformed univariate models and climatological benchmarks. For daily forecasts, the best model achieved NSE values close to 1 at a 1-day lead time and retained positive skill at longer horizons, while substantially reducing MAPE compared with the historical-average baseline. For weekly minimum low-flow forecasts, the LSTM models markedly improved NSE and MAPE relative to climatology at 1–2-week lead times, demonstrating clear added value for drought-relevant metrics. However, forecast skill degraded substantially at longer lead times, with NSE values becoming negative for some daily and weekly minimum, indicating that the models can perform worse than the mean of the observations when the forecast horizon is extended.

Overall, the results indicate that LSTM-based deep learning provides a powerful framework for sub-seasonal low-flow forecasting in the Rhine, particularly for short lead times of up to about 1–2 weeks. Within this horizon, the models capture the timing and magnitude of low-flow events more accurately than climatology and can support more proactive navigation management, water allocation, and drought preparedness in the downstream delta. Beyond this range, forecasts should be used cautiously and in combination with other sources of information.

Based on these findings, we recommend the following directions for further model development and application:

1. Broaden and refine predictor sets. Incorporate additional dynamic predictors (e.g., soil-moisture proxies, snow indicators, climate indices) and relevant static characteristics (e.g., physiographic descriptors) to better represent the processes controlling low flows.
2. Explore hybrid and comparative approaches. Combine LSTM architectures with other machine-learning models or process-based hydrological models to exploit complementary strengths and to benchmark deep-learning performance against existing Rhine forecasting systems.
3. Investigate sub-basin-scale and transfer learning applications. Extend the framework to individual Rhine sub-basins and assess the use of transfer learning or regionalization strategies to improve local skill and generalization to other basins with similar hydroclimatic regimes.
4. Enhance uncertainty characterization. Develop probabilistic LSTM-based forecasts (e.g., ensembles, Bayesian or quantile models) to better quantify predictive uncertainty, particularly for decision-making under low-flow conditions.
5. Integrate with operational products. Systematically compare LSTM-based forecasts with existing operational Rhine forecasts and evaluate how deep-learning outputs can be incorporated into current early-warning and river-management workflows.

Implementing these recommendations will help to further improve the robustness, interpretability, and operational value of LSTM-based sub-seasonal low-flow forecasting for the Rhine and other large river basins.

Institutional Review Board Statement: Not applicable. This study did not involve experiments on humans or animals.

Informed Consent Statement: Not applicable.

Data Availability Statement: The GRDC discharge data used in this study are available from the Global Runoff Data Centre (https://portal.grdc.bafg.de) under their data use terms. ERA5 reanalysis data are openly available from the Copernicus Climate Data Store (dataset "ERA5 hourly data on single levels from 1940 to present"). The processed basin-average input time series and LSTM model scripts are available from the corresponding author on reasonable request due to institutional restrictions.

Funding: This research received no external funding.

Conflicts of Interest: The authors declare no conflict of interest.

Author Contributions: Conceptualization, T.B.S.; methodology, T.B.S.; software, T.B.S.; validation, T.B.S.; formal analysis, T.B.S.; investigation, T.B.S.; visualization, T.B.S; data curation, T.B.S.; writing-original draft preparation, T.B.S.; writing-review and editing, S.K; All authors have read and agreed to the published version of the manuscript

Acknowledgments: The authors acknowledge the use of AI (copilot) for language editing support

Abbreviations

LSTM Long Short-Term Memory

RNN Recurrent Neural Network

GRDC Global Runoff Data Centre

ECMWF European Centre for Medium-Range Weather Forecasts

ERA5 ECMWF Reanalysis v5

NSE Nash–Sutcliffe Efficiency

MAPE Mean Absolute Percentage Error

SISO Single Input Single Output

SIMO Single Input Multiple Output

MISO Multiple Input Single Output

S2S Sub-seasonal to Seasonal

GPU Graphics Processing Unit

References

1. Van Loon, A.F. Hydrological drought explained. *WIREs Water* 2015, *2*, 359–392. https://doi.org/10.1002/wat2.1085
2. Palmer, W.C. *Meteorological Drought*; U.S. Weather Bureau Research Paper No. 45; U.S. Department of Commerce: Washington, DC, USA, 1965; p. 58. Available online: https://www.ncei.noaa.gov/pub/data/papers/Palmer_Drought_1965.pdf (accessed on 2 April 2026).
3. Demirel, M.C.; Booij, M.J.; Hoekstra, A.Y. Identification of appropriate lags and temporal resolutions for low flow indicators in the River Rhine to forecast low flows with different lead times. *Hydrol. Process.* 2013, *27*, 2742–2758. https://doi.org/10.1002/hyp.9402
4. Weiland, F.S.; Hegnauer, M.; Bouaziz, L.; Beersma, J. *Implications of the KNMI'14 Climate Scenarios for the Discharge of the Rhine and Meuse*; Deltares Report 1220042-000; Deltares: Delft, The Netherlands, 2015. Available online: http://publications.deltares.nl/1220042_000.pdf (accessed on 2 April 2026).
5. Wagenaar-Hart, A.M. International Commission for the Hydrology of the Rhine Basin (CHR). *Water Sci. Technol.* 1994, *29*, 375–378. https://doi.org/10.2166/wst.1994.0138
6. International Commission for the Protection of the Rhine (ICPR). *Inventory of the Low Water Conditions on the Rhine*; ICPR Report No. 248; ICPR: Koblenz, Germany, 2018. Available online: https://www.iksr.org (accessed on 2 April 2026).
7. Gauch, M.; Kratzert, F.; Klotz, D.; Nearing, G.; Lin, J. Data and physics-driven deep learning for hydrological model generalization. *Water Resour. Res.* 2021, *57*, e2021WR029640. https://doi.org/10.1029/2021WR029640
8. Chen, L.; Singh, V.P.; Lu, W.; Zhang, J.; Zhou, J.; Guo, S. Streamflow forecast uncertainty evolution and its effect on real-time reservoir operation. *J. Hydrol.* 2016, *540*, 712–726. https://doi.org/10.1016/j.jhydrol.2016.06.015
9. Duan, Q.; Pappenberger, F.; Wood, A.; Cloke, H.L.; Schaake, J.C. *Handbook of Hydrometeorological Ensemble Forecasting*; Springer: Berlin/Heidelberg, Germany, 2019; pp. 1–1528. https://doi.org/10.1007/978-3-642-39925-1
10. Fan, F.M.; Collischonn, W.; Meller, A.; Botelho, L.C.M. Ensemble streamflow forecasting experiments in a tropical basin: The São Francisco River case study. *J. Hydrol.* 2014, *519*, 2906–2919. https://doi.org/10.1016/j.jhydrol.2014.04.038
11. Shen, C. A transdisciplinary review of deep learning research and its relevance for water resources scientists. *Water Resour. Res.* 2018, *54*, 8558–8593. https://doi.org/10.1029/2018WR022643
12. Kratzert, F.; Klotz, D.; Brenner, C.; Schulz, K.; Herrnegger, M. Rainfall–runoff modelling using Long Short-Term Memory (LSTM) networks. *Hydrol. Earth Syst. Sci.* 2018, *22*, 6005–6022. https://doi.org/10.5194/hess-22-6005-2018
13. Fang, Z.; Wang, Y.; Peng, L.; Hong, H. Predicting flood susceptibility using Long Short-Term Memory (LSTM) neural networks. *J. Hydrol.* 2021, *594*, 125734. https://doi.org/10.1016/j.jhydrol.2020.125734

14. Lees, T.; Buechel, M.; Anderson, B.; Slater, L.; Dadson, S.; et al. (If you keep the Lees et al. citation, insert full details here—journal, year, volume, pages and DOI—using your existing reference or a database lookup.)
15. Hochreiter, S.; Schmidhuber, J. Long Short-Term Memory. *Neural Comput.* 1997, *9*, 1735–1780. https://doi.org/10.1162/neco.1997.9.8.1735
16. Hu, R.; Fang, F.; Pain, C.C.; Navon, I.M. Rapid spatio-temporal flood prediction and uncertainty quantification using a deep learning method. *J. Hydrol.* 2019, *575*, 911–920. https://doi.org/10.1016/j.jhydrol.2019.05.087
17. Barzegar, R.; Aalami, M.T.; Adamowski, J. Coupling a hybrid CNN–LSTM deep learning model with a boundary-corrected maximal overlap discrete wavelet transform for multiscale lake water level forecasting. *J. Hydrol.* 2021, *598*, 126196. https://doi.org/10.1016/j.jhydrol.2021.126196
18. Hauswirth, S.M.; Bierkens, M.F.P.; Beijk, V.; Wanders, N. The potential of data-driven approaches for quantifying hydrological extremes. *Adv. Water Resour.* 2021, *155*, 104017. https://doi.org/10.1016/j.advwatres.2021.104017
19. Rasouli, K.; Hsieh, W.W.; Cannon, A.J. Daily streamflow forecasting by machine learning methods with weather and climate inputs. *J. Hydrol.* 2012, *414–415*, 284–293. https://doi.org/10.1016/j.jhydrol.2011.10.039
20. Copernicus Climate Change Service (C3S); Climate Data Store (CDS). ERA5 hourly data on single levels from 1940 to present. *C3S Climate Data Store (CDS)*, 2023. Available online: https://cds.climate.copernicus.eu/cdsapp#!/dataset/reanalysis-era5-single-levels (accessed on 2 April 2026).
21. Hersbach, H.; Bell, B.; Berrisford, P.; Hirahara, S.; Horányi, A.; Muñoz-Sabater, J.; et al. The ERA5 global reanalysis. *Q. J. R. Meteorol. Soc.* 2020, *146*, 1999–2049. https://doi.org/10.1002/qj.3803
22. Beck, H.E.; et al. Biases and trends in ERA5 precipitation reanalysis across global hydroclimates. *Atmosphere* 2023, *14*, 826. https://doi.org/10.3390/atmos14070826
23. Mizukami, N.; Clark, M.P.; Slater, A.G.; Brekke, L.D.; Elsner, M.M.; Arnold, J.R.; Gangopadhyay, S. Hydrologic implications of different large-scale meteorological forcings in global water resource simulations. *Water Resour. Res.* 2017, *53*, 7973–7992. https://doi.org/10.1002/2017WR020452
24. GRDC (Global Runoff Data Centre). *GRDC Data Portal*; Federal Institute of Hydrology (BfG): Koblenz, Germany, 2021. Available online: https://portal.grdc.bafg.de (accessed on 2 April 2026).
25. Nearing, G.S.; Addor, N.; Newman, A.J.; Gupta, H.V.; Clark, M.P. What role does hydrologic model complexity play in learning from data? *Water Resour. Res.* 2021, *57*, e2020WR028091. https://doi.org/10.1029/2020WR028091

Supplementary Materials

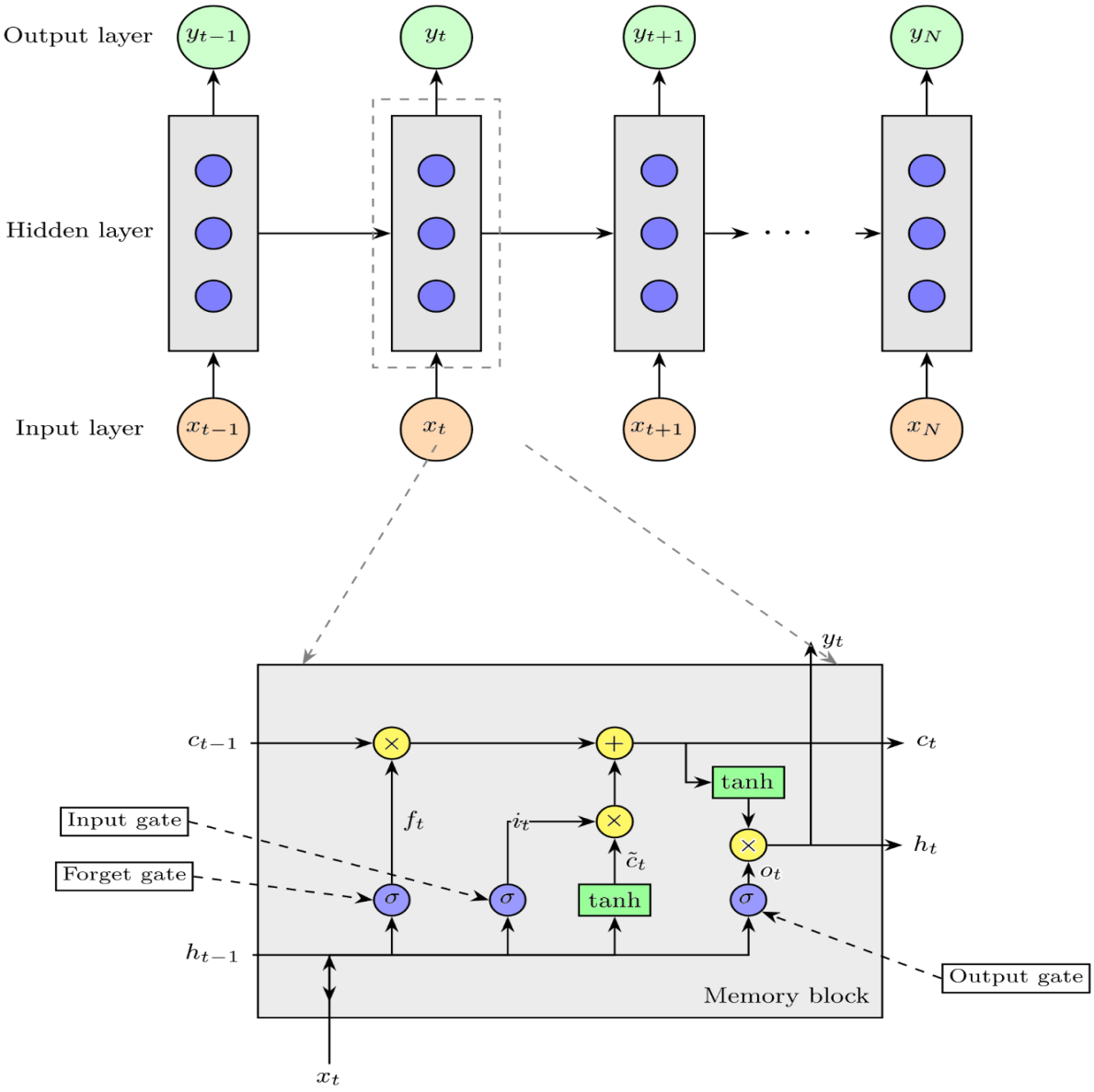

Figure 1A The structure of the cell connection in the long short-term memory neural network

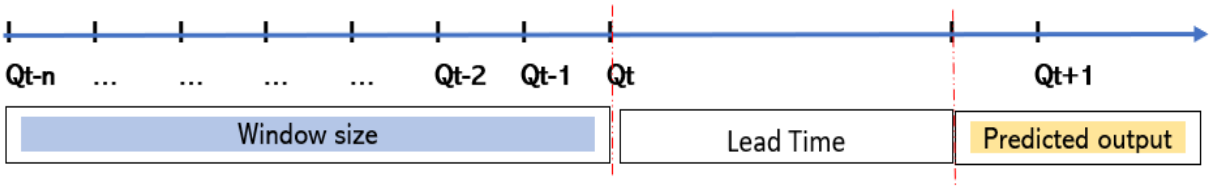

Figure 2A Graphical representation of the window size and predicted output with corresponding lead time

In this analysis, Q(t) represents the streamflow at time t, and we use the vector (Q(t − n), …, Q(t)) as the input in the subsequent step to predict the value Q(t+1).